CONCRETE LIBRARY OF JSCE NO. 32, DECEMBER 1998

STUDY ON A METHOD OF OBTAINING YIELD VALUES OF FRESH CONCRETE FROM SLUMP FLOW TEST

(Translation from Proceedings of JSCE, No.578/V-37, November 1997)

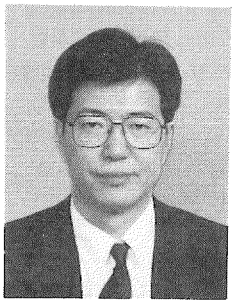
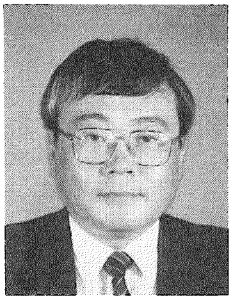
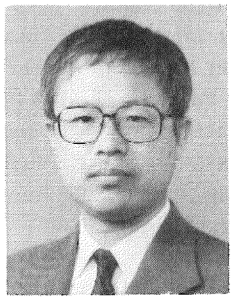
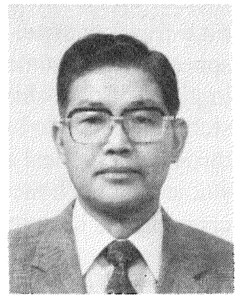

Takeshi KOKADO Takashi HOSODA Toyoaki MIYAGAWA Manabu FUJI

An equation that expresses the flow behavior of high-flow concrete in the slump flow test is derived from basic equations of fluids and, at the same time, a theoretical equation expressing the relationship between slump flow and yield value is developed from this equation describing flow behavior. The validity of the derived theoretical equation is verified by conducting slump flow tests and sphere drag tests.

Key Words: *Slump flow, flowability, high-flow concrete, self-placing concrete, rheology, Bingham plastics, yield value*

Takeshi KOKADO is a manager in the Construction Materials Development Div. at Nippon Steel Corporation. His research interests relate to the rheology of fresh concrete and the application of high-flow concrete to steel-concrete composite structures for submerged tunnel caissons and shield tunnel segments. He is a member of the JCI and JSCE.

Takashi HOSODA is an Associate Professor in the Department of Civil Engineering at Kyoto University, Kyoto, Japan. He received his Doctor of Engineering Degree from Kyoto University in 1990. He is the author of a number of papers dealing with open channel hydraulics, turbulent flows, and river channel processes. He is a member of the IAHR, JSFM, JSCFD, and JSCE.

Toyoaki MIYAGAWA is a Professor in the Department of Civil Engineering at Kyoto University, Kyoto, Japan. He received his Doctor of Engineering Degree from Kyoto University in 1985. He is the author of a number of papers dealing with the durability, maintenance, and repair of reinforced concrete structures. He is a member of the ACI, RILEM, fib, JSMS, JCI, and JSCE.

Manabu FUJI was a Professor in the Department of Civil Engineering at Kyoto University, Kyoto, Japan. He received his Doctor of Engineering Degree from Kyoto University in 1972. His research activities were focused on the optimal design of prestressed concrete cable-stayed bridges, structural safety evaluations, and the durability of concrete structures. He has written some 50 papers on these subjects. He was a member of the ACI, JSMS, JCI, and JSCE.

1. INTRODUCTION

To accomplish labor saving and rationalization in the execution of concrete work, high-flow concretes with excellent fluidity, such as self-placing concrete [1], have been developed and put into practical use. Slump flow is widely used in the laboratory and in the field as an index of the fluidity of such high-flow concretes.

Studies on the rheology of fresh concrete have been carried out since before the development of high-flow concrete. Measurements of the rheological coefficients using rotational viscometers, sphere drag viscometers, etc. have demonstrated that the rheological properties of fresh concrete imply the flow behavior of Bingham plastics [2], [3]. Attempts have been made to express the slump of concrete by associating it with the rheological coefficients (yield value, plastic viscosity) through theoretical analysis and numerical analysis [4], [5], [6]. However, there have been few studies in which the relationship between slump flow and rheological coefficients for high-flow concrete has been investigated [7], [8].

If slump flow could be theoretically expressed as a function of rheological coefficients, it would become possible to clarify the rheological significance of slump flow, which is used as an index of the fluidity of high-flow concrete.

In this study, the relationship between slump flow and the yield value of high-flow concrete is theoretically discussed. At the same time, the validity and usefulness of the theoretical equation obtained as a result of this discussion are demonstrated by conducting a series of slump flow tests and sphere drag tests.

2. THEORETICAL DISCUSSION

An equation that expresses the flow behavior of high-flow concrete in the slump flow test using a slump cone on a flow table is derived from basic fluid equations. Further, a theoretical equation that expresses the relationship between slump flow and yield value is derived from this equation of flow behavior.

(1) Basic Equations

The motion of a fluid is generally expressed by combining an equation of continuity and an equation of motion. In the case of an incompressible fluid, the equation of continuity and the equation of motion (r component) are expressed in cylindrical coordinates (r, θ, z) as follows.

Equation of continuity:

$$\frac{1}{r}\frac{\partial}{\partial r}(r v_r)+\frac{1}{r}\frac{\partial v_\theta}{\partial \theta}+\frac{\partial v_z}{\partial z}=0 \qquad (1)$$

Equation of motion (r component) :

$$\frac{\partial v_r}{\partial t}+v_r\frac{\partial v_r}{\partial r}+\frac{v_\theta}{r}\frac{\partial v_r}{\partial \theta}+v_z\frac{\partial v_r}{\partial z}-\frac{v_\theta^{2}}{r}=-\frac{1}{\rho}\frac{\partial p}{\partial r}+\frac{1}{\rho}\left(\frac{1}{r}\frac{\partial}{\partial r}(r\tau_{rr})+\frac{1}{r}\frac{\partial \tau_{\theta r}}{\partial \theta}-\frac{\tau_{\theta\theta}}{r}+\frac{\partial \tau_{zr}}{\partial z}\right)+g_r \qquad (2)$$

Here, v_r, v_θ, v_z are the components of the velocity vector, τ_{ij} is the stress tensor, ρ is density, p is pressure, g_r (=0) is the r direction component of gravitational acceleration, and t is time.
As a matter of interest, the left side of Eq. (2) gives an inertia term, while the first term of its right side is a pressure term and the second a viscosity term.
Therefore, the flow at any one point in a concrete specimen is governed by Eqs. (1) and (2)

throughout the period from cone removal until the specimen becomes stationary.

(2) Integration of Equation of Continuity

The equation of continuity (1) is integrated from the base of the specimen up to the free surface during flow, h:

$$\int_0^h \frac{\partial}{\partial r}(rv_r)dz + \int_0^h \frac{\partial v_\theta}{\partial \theta}dz + \int_0^h r\frac{\partial v_z}{\partial z}dz = 0 \qquad (3)$$

Equation (4) can be obtained using Eq. (3) by applying Leibnitz's rule [9] on the assumption that the base is horizontal.

$$\frac{\partial}{\partial r} r\int_0^h v_r dz - rv_{r_s}\frac{\partial h}{\partial r} + \frac{\partial}{\partial \theta}\int_0^h v_\theta dz - v_{\theta_s}\frac{\partial h}{\partial \theta} + rv_{z_s} - rv_{z_b} = 0 \qquad (4)$$

Here, the subscripts s and b affixed to the components of the velocity vector denote the free surface and the base, respectively, of the specimen.

If the average velocity of the component in the r direction and the θ direction from the free surface to the base is u_r and u_θ, respectively, then the following equations hold:

$$u_r = \frac{1}{h}\int_0^h v_r dz \qquad (5)$$

$$u_\theta = \frac{1}{h}\int_0^h v_\theta dz \qquad (6)$$

Also, from the free surface condition, the following equation holds:

$$v_{z_s} = \frac{\partial h}{\partial t} + v_{r_s}\frac{\partial h}{\partial r} + \frac{v_{\theta_s}}{r}\frac{\partial h}{\partial \theta} \qquad (7)$$

Rearranging Eq. (4) using Eqs. (5), (6), and (7), we obtain

$$r\frac{\partial h}{\partial t} + \frac{\partial}{\partial r}(ru_r h) + \frac{\partial}{\partial \theta}(u_\theta h) - rv_{z_b} = 0 \qquad (8)$$

Because the flow (spread) of concrete is of interest in the slump flow test, the flow in question is axisymmetric. The flow spreads radially from the origin, and no outflow nor inflow of concrete from the base (flow table) occurs. Therefore, the following equations hold:

$$\frac{\partial}{\partial \theta} = 0 \qquad (9)$$

$$v_{z_b} = 0 \qquad (10)$$

Consequently, the equation of continuity integrated from the base to the height of the free surface of a specimen during flow, is as follows.

$$\frac{\partial h}{\partial t} + \frac{1}{r}\frac{\partial}{\partial r}(ru_r h) = 0 \qquad (11)$$

(3) Integration of Equation of Motion

a) Inertia Term

Rearranging the inertia term of the equation of motion (2) using the equation of continuity (1), we obtain Eq. (12).

$$\text{Inertia term} = \frac{\partial v_r}{\partial t} + \frac{1}{r}\frac{\partial}{\partial r}\left(rv_r^{\,2}\right) + \frac{1}{r}\frac{\partial}{\partial \theta}(v_r v_\theta) + \frac{\partial}{\partial z}(v_r v_z) - \frac{v_\theta^{\,2}}{r} \qquad (12)$$

The inertia term, Eq. (12), is integrated from the base to the free surface of the specimen during flow.

$$\int_0^h (inertia\ term)dz = \int_0^h \left(\frac{\partial v_r}{\partial t} + \frac{1}{r}\frac{\partial}{\partial r}\left(r v_r^{\ 2}\right) + \frac{1}{r}\frac{\partial}{\partial \theta}\left(v_r v_\theta\right) + \frac{\partial}{\partial z}\left(v_r v_z\right) - \frac{v_\theta^{\ 2}}{r} \right) dz \qquad (13)$$

As with the equation of continuity, Eq. (14) is obtained by applying Leibnitz's rule and using Eqs. (5), (7), (9), and (10).

$$\int_0^h (inertia\ term)dz = \frac{\partial}{\partial t}\left(u_r h\right) + \frac{1}{r}\frac{\partial}{\partial r} r \int_0^h v_r^{\ 2} dz \qquad (14)$$

If we substitute Eq. (15), in which the momentum correction coefficient β is introduced,

$$\frac{1}{h}\int_0^h v_r^{\ 2} dz = \beta u_r^{\ 2} \qquad (15)$$

then Eq. (14) can be rewritten as Eq. (16):

$$\int_0^h (inertia\ term)dz = \frac{\partial}{\partial t}\left(u_r h\right) + \frac{1}{r}\frac{\partial}{\partial r}\left(r \beta u_r^{\ 2} h\right) \qquad (16)$$

b) Pressure Term

Next, the pressure term is integrated in the height direction.

$$\int_0^h (pressure\ term)dz = -\frac{1}{\rho}\int_0^h \frac{\partial p}{\partial r} dz \qquad (17)$$

By Leibnitz's rule,

$$\int_0^h (pressure\ term)dz = -\frac{1}{\rho}\frac{\partial}{\partial r}\int_0^h p dz + \frac{1}{\rho} p_s \frac{\partial h}{\partial r} \qquad (18)$$

If the pressure, p, at height z from the base is assumed to have a static pressure distribution, then

$$p = \rho g (h - z) \qquad (19)$$

Here, g is gravitational acceleration.
Also, on the surface of specimen,

$$p_s = 0 \qquad (20)$$

Therefore, the pressure term of the equation, when integrated from the base to the height of the free surface of the specimen during flow, becomes Eq. (21):

$$\int_0^h (pressure\ term)dz = -gh\frac{\partial h}{\partial r} \qquad (21)$$

c) Viscosity Term

Similarly, the viscosity term is integrated in the height direction.

$$\int_0^h (vis\cos ity\ term)dz = \frac{1}{\rho}\int_0^h \left(\frac{\partial \tau_{rr}}{\partial r} + \frac{1}{r}\frac{\partial \tau_{\theta r}}{\partial \theta} + \frac{\partial \tau_{zr}}{\partial z} - \frac{\tau_{\theta\theta}}{r} + \frac{\tau_{rr}}{r} \right) dz \qquad (22)$$

Carrying out calculations using Leibnitz's rule, we obtain:

$$\int_0^h (vis\cos ity\ term)dz = \frac{1}{\rho}\frac{\partial}{\partial r}\int_0^h \tau_{rr} dz - \frac{1}{\rho}\tau_{rr_s}\frac{\partial h}{\partial r} + \frac{1}{\rho r}\frac{\partial}{\partial \theta}\int_0^h \tau_{\theta r} dz - \frac{1}{\rho r}\tau_{\theta r_s}\frac{\partial h}{\partial \theta}$$

$$+\frac{\tau_{zr_s}}{\rho} - \frac{\tau_{zr_b}}{\rho} - \frac{1}{\rho r}\int_0^h \tau_{\theta\theta} dz + \frac{1}{\rho r}\int_0^h \tau_{rr} dz \qquad (23)$$

Since there is no stress acting on the surface (that is, the stress vector acting on the surface is assumed to be 0), the following equation is obtained:

$$\tau_{zr_s} - \tau_{rr_s}\frac{\partial h}{\partial r} - \frac{1}{r}\tau_{\theta r_s}\frac{\partial h}{\partial \theta} = 0 \qquad (24)$$

Also, the following equation is obtained from Eq. (9):

$$\frac{1}{\rho r}\frac{\partial}{\partial\theta}\int_0^h \tau_{\theta r}dz = 0 \tag{25}$$

Furthermore, if the r component of the stress vector acting on the base is τ_{b_r}, then because the base is horizontal, the following equation holds:

$$\tau_{b_r} = \tau_{zr_b} \tag{26}$$

Therefore,

$$\int_0^h (viscosity\ term)dz = \frac{1}{\rho}\frac{\partial}{\partial r}\int_0^h \tau_{rr}dz - \frac{1}{\rho r}\int_0^h \tau_{\theta\theta}dz + \frac{1}{\rho r}\int_0^h \tau_{rr}dz - \frac{\tau_{b_r}}{\rho} \tag{27}$$

The normal stresses τ_{rr} and $\tau_{\theta\theta}$ are expressed by Eq. (28) and Eq. (29), respectively, in the case of an incompressible fluid.

$$\tau_{rr} = 2\eta\frac{\partial v_r}{\partial r} \tag{28}$$

$$\tau_{\theta\theta} = 2\eta\left(\frac{1}{r}\frac{\partial v_\theta}{\partial\theta} + \frac{v_r}{r}\right) \tag{29}$$

Where η is viscosity.

In the case of Bingham plastics, viscosity η is expressed by Eq. (30).

$$\eta = \eta_{pl} + \frac{\tau_y}{2\sqrt{I_2}} \tag{30}$$

Here, η_{pl} is plastic viscosity and I_2 is the secondary invariant of the strain rate tensor.

Substituting Eqs. (28) and (29) into Eq. (27), we obtain

$$\int_0^h (viscosity\ term)dz = \frac{1}{\rho}\frac{\partial}{\partial r}\int_0^h 2\eta\frac{\partial v_r}{\partial r}dz - \frac{1}{\rho r^2}\int_0^h 2\eta v_r dz + \frac{1}{\rho r}\int_0^h 2\eta\frac{\partial v_r}{\partial r}dz - \frac{\tau_{b_r}}{\rho} \tag{31}$$

d) Equation of Motion Integrated in Height Direction

Accordingly, the full equation of motion integrated from the base to the height of the free surface of the specimen during flow can be expressed by Eq. (32).

$$\frac{\partial}{\partial t}(u_r h) + \frac{1}{r}\frac{\partial}{\partial r}\left(r\beta u_r{}^2 h\right) = -gh\frac{\partial h}{\partial r} + \frac{1}{\rho}\frac{\partial}{\partial r}\int_0^h 2\eta\frac{\partial v_r}{\partial r}dz - \frac{1}{\rho r^2}\int_0^h 2\eta v_r dz + \frac{1}{\rho r}\int_0^h 2\eta\frac{\partial v_r}{\partial r}dz - \frac{\tau_{b_r}}{\rho} \tag{32}$$

(4) Proposal of Theoretical Equation

Noting that the concrete enters a stationary after flow, we obtain

$$u_r = 0 \tag{33}$$

$$v_{r_s} = 0 \tag{34}$$

Since it can be considered that the shear stress at the bottom of the specimen when at rest is equal to the yield value of the fresh concrete τ_y, the following equation holds:

$$\tau_{b_r} = \tau_y \tag{35}$$

Therefore, the inertia term and part of the viscosity term of equation of motion (32) integrated in the height direction become 0, and Eq. (36) holds in a condition in which the concrete has come to rest in the slump flow test:

$$-gh\frac{\partial h}{\partial r} - \frac{\tau_y}{\rho} = 0 \tag{36}$$

Equation (36) is then integrated, and the following boundary condition is given:

$$r=L\ ;\ h=0 \tag{37}$$

Where L is the distance from the center to the edges of the specimen.

Then, a theoretical equation (38) is derived which expresses the height distribution of the specimen once the concrete has come to rest after flow in the slump flow test.

$$\frac{h^2}{2}=(L-r)\frac{\tau_y}{\rho g} \tag{38}$$

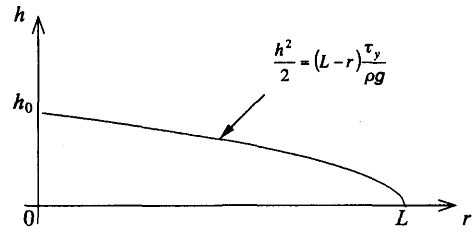

Fig.1 Height distribution of specimen derived from theoretical equation (38)

Equation (38) demonstrates that the height distribution of a specimen after the slump flow test describes a parabola **(Fig.-1)**.

If the height of the center of specimen (r = 0) is h_0, then Eq. (39) can be derived, and the yield value of the fresh concrete τ_y is given by L and h_0.

$$\tau_y=\frac{\rho g h_0{}^2}{2L} \tag{39}$$

The volume of specimen, V, can be given by Eq. (40) using Eqs. (38) and (39).

$$V=\int_0^{h_0}\pi r^2 dh=\frac{8\pi L^2 h_0}{15} \tag{40}$$

From Eqs. (39) and (40), therefore, the yield value of the fresh concrete τ_y is expressed by Eq. (41) as a function of slump flow, Sf(= 2L).

$$\tau_y=\frac{15^2\rho g V^2}{4\pi^2 Sf^5} \tag{41}$$

3. EXPERIMENTAL CONDITIONS

(1) Outline of Experiment

In order to evaluate the suitability of equation (41), which theoretically expresses the relationship between slump flow and the yield value of fresh concrete, simultaneous measurements of slump flow and rheological coefficients were made.

A sphere drag viscometer [10] suitable for the measurement of relatively soft specimens was used to measure the rheological coefficients. The experiment was conducted using mortar in which the only aggregate used was a fine one ; this minimized the size of the apparatus required, since the diameter of the sphere must be not less than 3 times the maximum aggregate size and the diameter of the container not less than 5 times the diameter of the sphere [11].

(2) Materials Used and Mix Proportion

A list of the materials used is given in **Table 1.** The binder is a mixture of ordinary Portlant cement (OPC) and ground granulated blast-furnace slag (BFS) at a weight ratio of 3 to 7 [12]. The fine aggregate is a mixture of Soma sand (silica sand) No. 3, No. 4, and No. 6, in equal quantities. The fine aggregate-binder ratio (S/B) was fixed at 1.50 in consideration of typical mix proportions for

Table 1 Materials used

Binder	Ordinary Portland cement (OPC) Density: 3.16×10^{-3} g/mm^3 Blaine's specific surface area: 3,270 cm^2/g
	Ground granulated blast-furnace slag (BFS) SO_3: 2.0% Density: 2.89×10^{-3} g/mm^3 Blaine's specific surface area: 6,020 cm^2/g
Fine aggregate	Soma sand (S) No. 3: No. 4: No. 6 = 1:1:1 Density: 2.60×10^{-3} g/mm^3, F.M.: 2.47
Viscous agent	Cellulose ether base (MC)
Super plasticizer	[Powder base] Naphthalenesulfonic acid base (SP1) [With viscous agent] Polycarboxylic acid base (SP2)

Table 2 List of mix proportions

Mix Proportion No.		W/B (%)	S/B	Air (%)	Quantity of material per unit volume (kg/m3) W	OPC	BFS	S	MC	SP
Powder base W/B=35%	1									6.966
	2									7.740
	3	35			271	232	542	1161		8.514
	4									10.062
	5								–	11.610
Powder base W/B=40%	1									2.232
	2									3.720
	3	40	1.5	2.15	298	223	521	1116		5.952
	4									7.440
	5									8.184
With viscous agent W/B=35%	1									7.740
	2	35			271	232	542	1161	0.678	11.610
	3									15.480
	4									19.350

various kinds of high-flow concrete[13].

Three mix proportions were tested, with water-binder ratios (W/B) of 35% and 40%, and a W/B of 35% plus a viscous agent added in an amount corresponding to 0.25% of water volume. In each of these mixtures, fluidity was adjusted by changing the amount of super plasticizer (SP). **Table 2** shows the mix proportions of these mixtures. A dual-spindle mixer was used to mix the mortar (volume: 50 *l*; speed: 62 rpm). After dry-mixing the binding materials and fine aggregate for 15 minutes, the water and super plasticizer were added and mixed for 2 minutes.

Figure 2 shows changes in slump flow with time when the amount of added SP is 10.06 kg/m^3 (W/B = 35%), 7.44 kg/m^3 (W/B = 40%), and 11.61 kg/m^3 (with viscous agent). It is apparent from this figure that with each mix proportion the slump flow begins to stabilize 15 minutes after the completion of mixing, and then scarcely changes over the following 30 minutes.

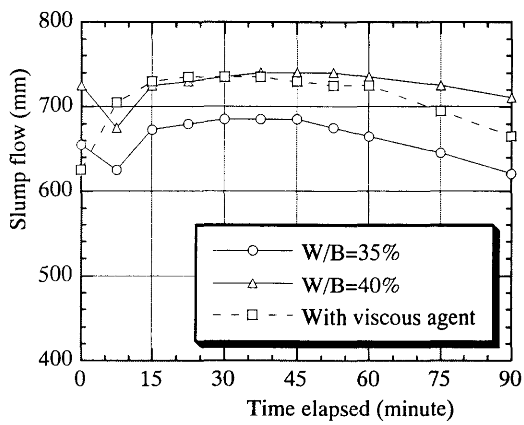

Fig. 2 Changes in slump flow with time

(3) Slump Flow Test

a) Test Method

Slump flow tests were conducted in accordance with JSCE-F503 using a slump cone as specified in JIS A 1101 and a steel-plate flow table measuring 1,000 mm in on a side. Samples were not tamped with a tamping rod when filling the cone, because the test covers the high-flow region, in which the cone is filled under the deadweight of the sample only. Drips of mortar falling after the cone was removed were collected in a dish in order to prevent this mortar dropping onto the specimen. Slump flow was measured to the nearest 1 mm. The height distribution (r, h) of each specimen was measured at a 20-mm pitch along the same line used to measure slump flow. Furthermore, the volume of the specimen was determined by measuring its weight. From the results of the prior measurement of changes in slump flow with time (**Fig. 2**), it was decided to start the test 15 minutes after completing mixing, when slump flow begins to stabilize.

b) Method of Data Analysis

The yield value τ_{yF} was found by substituting the slump flow and specimen volume into theoretical equation (41). From the measured values of height distribution (r, h) of each specimen, the yield value τ_{yR} was obtained by carrying out a regression analysis using L and τ_y as fitting parameters on the basis of the result expressed by the theoretical analysis of Eq. (38); that is, that the height distribution of a specimen is given by a parabola.

(4) Sphere Drag Test

a) Test Method

The arrangement of the sphere drag viscometer used to measure the rheological coefficients of the mortar sample is shown in **Fig. 3**. The diameter D of the steel sphere (JIS B 1501) is 19.05 mm and the diameter of the container is 284 mm. The sample mortar was placed to a height of 250 mm from the bottom of the container. The test began 15 minutes after the completion of mixing, as in the slump flow test, and was competed within 20 minutes. The sphere was pulled up from a point 50 mm above the bottom of the container, and the pull-up speed was constant throughout each measurement. The displacement y(t) of the sphere was measured using an ultrasonic displacement sensor, the drag force F(t) generated as the sphere was pulled was measured using a load cell, and all measurements were fed into the personal computer. The measurement interval was chosen in consideration of the sphere pull-up speed such that measurements would be obtained by the computer for each 1 mm of sphere travel. Motor speed was adjusted in advance such that the sphere pull-up speed became 5, 10, 15, 20, 25, and 30 mm/s. The measurement of each sample began at 5 mm/s, and measurements up to 30 mm/s were implemented by raising the speed by 5 mm/s each time. Then measurements were repeated by reducing the speed in 5 mm/s increments. This means that a total of 12 measurements were carried out for each sample within 20 minutes.

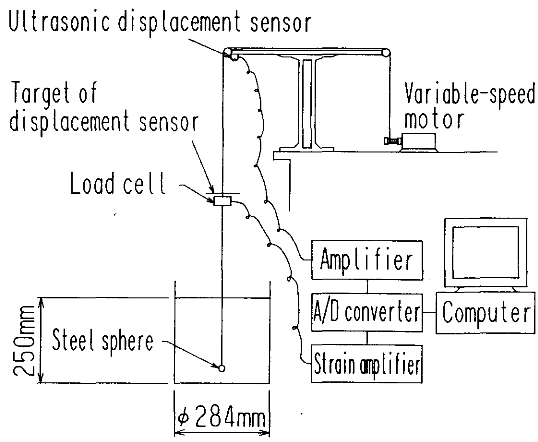

Fig.3 Sphere drag viscometer

The relationship between drag force F and sphere pull-up speed v was obtained from the mean value of the measured results (N: about 50) between 50 and 100 mm.

b) Method of Data Analysis

Ansley et al. [14] derived an equation that expresses the relationship between the drag force F acting on a sphere moving at a constant speed in a Bingham plastic, the yield value τ_y, and the plastic viscosity η_{pl}. At the same time, it was ascertained from the results of a falling ball test that Eq. (42) holds when the drag coefficient C_D, given by Eq. (43), is in the range 10^0 to 10^3.

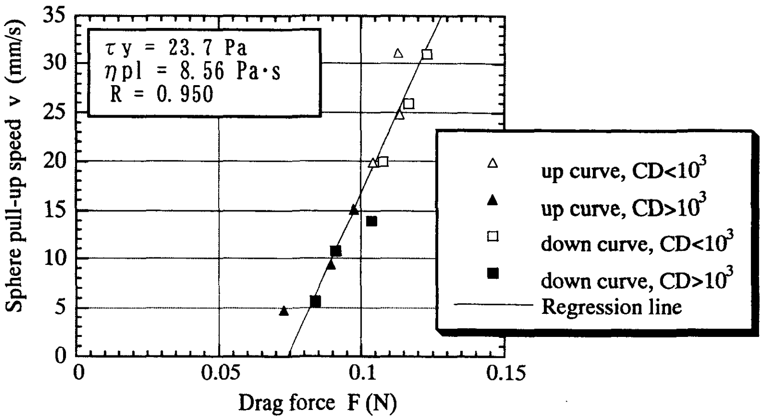

Fig. 4 Example of sphere drag test result

$$F = 3\pi D^2 \left(\eta_{pl} \frac{v}{D} + \frac{7\pi}{24} \tau_y \right) \tag{42}$$

$$C_D = \frac{8F}{\rho v^2 \pi D^2} \tag{43}$$

In the present experiment, the drag coefficient C_D is in the range 10^2 to 10^5, and measured values obtained when C_D exceeds 10^3 are also included in the results. As shown in **Fig. 4**, however, it was ascertained that even if the drag coefficient C_D, exceeds 10^3, a proportional relation is maintained between drag force F and sphere pull-up speed v. Therefore, it was decided to determine the yield value τ_{yD} and plastic viscosity η_{plD} from all measured values of F and v for each sample by linear regression using the method of least squares on the basis of Eq. (42).

4. Discussion of Experimental Results and Evaluation of Theoretical Equation

Table 3 shows the results of the slump flow tests and sphere drag tests, along with those of the regression analysis of height distribution.
The validity and effectiveness of the theoretical equation are examined on the basis of these experimental results.

(1) Height Distribution of Specimens

An example of a regression curve of height distribution as obtained from a slump flow test is shown in **Fig. 5**. In this sample of W/B = 40%-No.1 whose slump flow is 425 mm, there are portions between the center of the specimen (r = 0) and a radius of 100 mm where the measured value of height is not in agreement with the regression curve. In specimens with a slump flow of not less than 450 mm, however, the measured values of height are in good agreement with the regression curves.
From the relationship between slump flow and correlation coefficient shown in **Fig. 6**, it is apparent

Table 3 Overview of experimental results

Mix proportion No.		Slump flow test: Slump flow Sf (mm)	Height of center of specimen h_0 (mm)	Volume of specimen V ($\times 10^6$ mm^3)	Yield value τ_{yF} (Pa)	Regression analysis of height distribution: Correlation coefficient R	$2L$ (mm)	Yield value τ_{yR} (Pa)	h_{0R} (mm)	Sphere drag test: Yield value τ_{yD} (Pa)
W/B =35%	1	458	51.6	4.775	139.5	0.979	454	132.9	52.8	132.9
	2	468	48.5	4.684	120.5	0.976	464	115.9	49.9	107.5
	3	550	35.3	4.699	54.1	0.979	554	49.5	35.6	55.5
	4	673	27.5	4.866	21.1	0.988	672	22.8	26.6	31.0
	5	835	16.0	4.609	6.5	0.995	840	6.8	16.4	15.1
W/B =40%	1	425	66.3	5.429	256.5	0.964	430	260.1	71.1	240.4
	2	508	45.1	4.950	87.4	0.983	502	86.9	45.5	88.9
	3	663	26.9	5.031	23.8	0.985	664	22.9	26.8	29.5
	4	730	24.3	5.071	15.0	0.988	728	15.5	23.1	23.7
	5	810	20.6	5.041	8.8	0.993	804	9.9	19.4	12.2
With viscous agent W/B=35%	1	543	31.0	4.173	45.5	0.983	538	41.5	31.7	55.5
	2	740	18.5	4.404	10.8	0.984	750	10.7	19.3	19.5
	3	823	15.5	4.482	6.6	0.991	822	6.9	16.2	11.4
	4	905	14.0	4.689	4.5	0.991	914	4.6	14.0	4.3

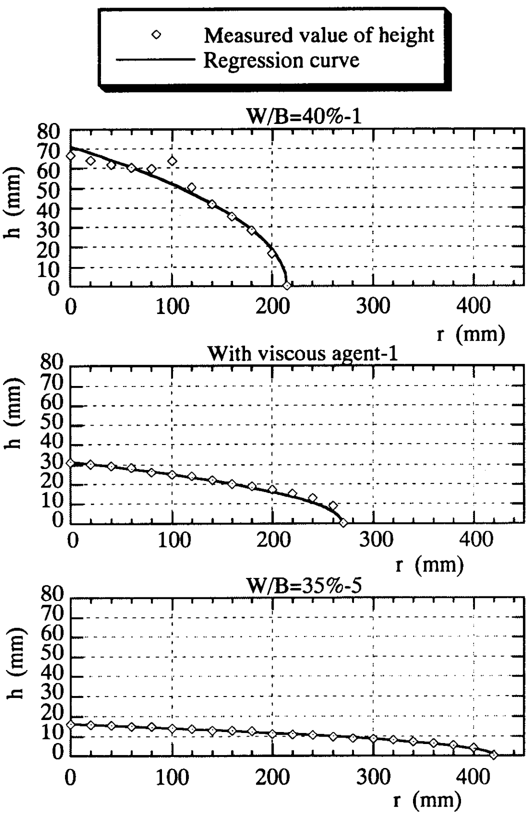

Fig. 5 Regression curve of height distribution

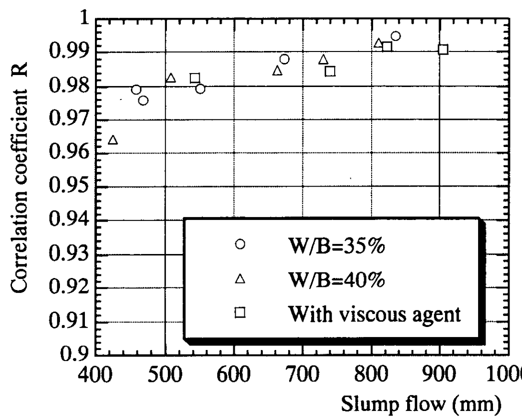

Fig. 6 Relationship between slump flow and correlation coefficient

that if slump flow is at least 450 mm, the height distribution of a specimen can be approximated with a considerably high correlation (correlation $\geqq$ 0.98) by a parabola. Furthermore, as shown in **Fig. 7**, the measured value of height at the center of a specimen (h_0) is in most cases in good agreement with the calculated value at $r = 0$ (h_{0R}), as obtained by substituting L obtained from the regression analysis and the yield value τ_{yR}, into Eq. (38). The exception is case W/B = 40%-No.1.

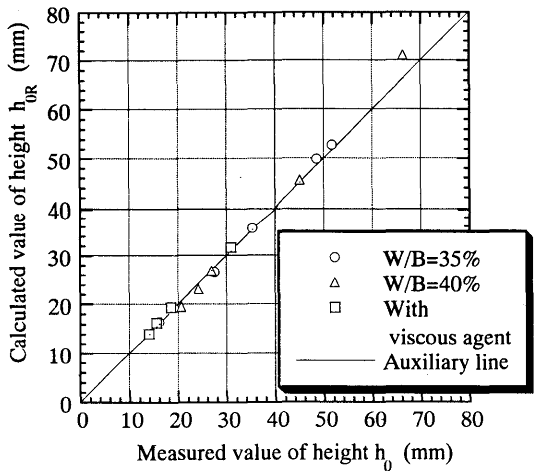

Fig. 7 Comparison between measured and calculated values of height of center of specimen

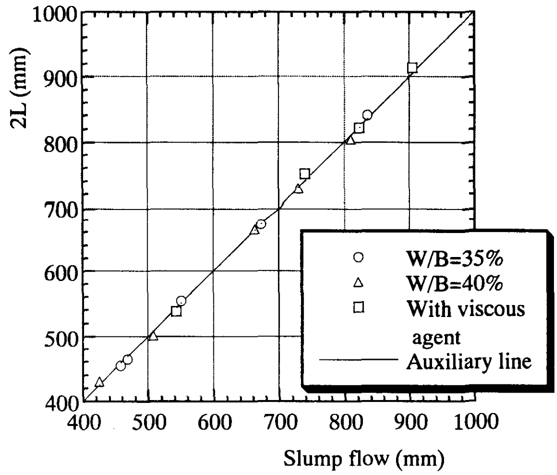

Fig. 8 Comparison between slump flow and *2L*

As shown in **Fig. 8**, the slump flow agrees well with *2L* in all cases. Accordingly, it is verified that the results of regression analysis of the height distribution of specimens in the slump flow tests based on Eq. (38) derived from theoretical analysis are in good agreement with measured values when the slump flow is at least 450 mm.

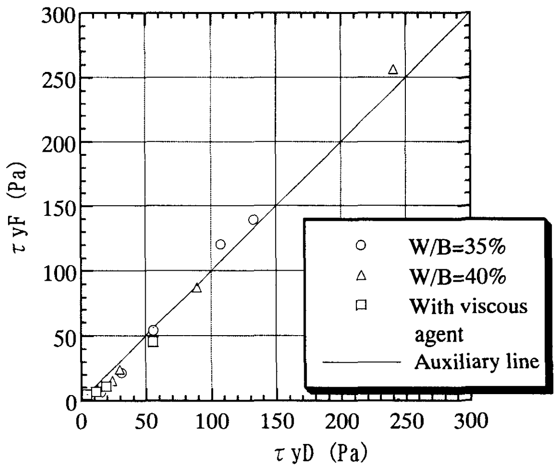

Fig. 9 Comparison of results of of yield value measurements

(2) Comparison with Results of Sphere Drag Test

Figure 9 shows the relationship between the yield value τ_{yF} as found using the theoretical equation (41) from the slump flow and the specimen volume, and the yield value τ_{yD} found from the sphere drag test. This figure shows that τ_{yD} takes somewhat higher values than τ_{yF} does in the region where the yield value is up to 100 Pa, while τ_{yF} takes somewhat higher values than τ_{yD} does in the region above 100 Pa. Thus, τ_{yF} is in agreement with τ_{yD} to an accuracy good enough for practical use over the wide range from 0 to about 250 Pa.

This demonstrates that the yield value can be obtained with considerably high accuracy from the slump flow as obtained from a slump flow test and the volume of the specimen.

(3) Normalization of Slump Flow

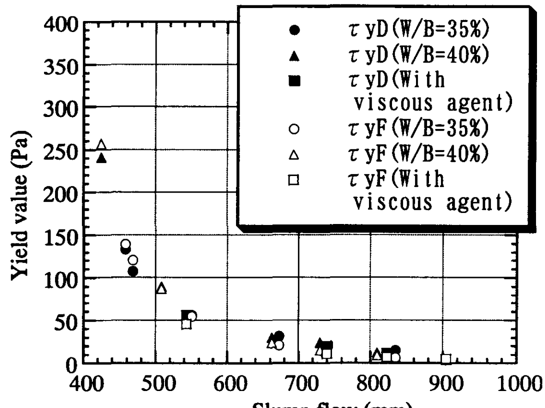

Fig. 10 Relationship between slump flow and yield value

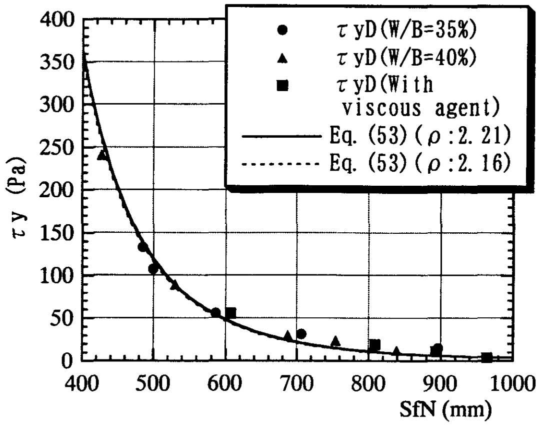

Fig. 11 Relationship between normalized slump flow and yield value

Figure 10 shows the relationship between slump flow and yield values τ_{yF} and τ_{yD} as found above. The yield value found from Eq. (41), τ_{yF}, is not only a function of slump flow, but also depends on the volume of the specimen. In these experiments, to prevent mortar left within the cone from dropping onto the specimen after pulling up the cone, a dish was used to collect the drippings. For this reason, the volume of specimen has a smaller volume than the slump cone by the amount of mortar left in the cone, as shown in **Table 3.** Besides, the volume varies a little from one slump flow test to another. Therefore, in order to find the relationship between slump flow and yield value for a constant specimen volume (= the volume of slump cone), the slump flow was normalized using Eq. (44) obtained by reference to Eq. (41).

$$Sf_N = \left(\frac{V_N}{V}\right)^{\frac{2}{5}} \times Sf \qquad (44)$$

Here Sf_N is the normalized slump flow (mm) and V_N is the volume of the slump cone ($1.75\pi \times 10^6$ mm^3).

The relationship between normalized slump flow Sf_N and yield value is shown in **Fig. 11**. By normalizing the slump flow in this way, it is possible to more clearly express the relationship between slump flow and yield value using theoretical equation (41).

5. Summary

(1) Proposal of Theoretical Equation

An equation that expresses the flow behavior of concrete in the slump flow test (Eq. (32)) was derived from continuity and motion equations. By noting that concrete reaches a stationary state after flow finishes, a theoretical equation for the height distribution of a specimen after the slump flow test (Eq. (38)) and another that gives the relationship between slump flow and yield value (Eq. (41)) were developed from the derived equation.

(2) Verification by Experiment

Slump flow tests and sphere drag tests were carried out on mortar, and as a result the following points were verified:

a)When the slump flow is at least 450 mm, a regression of the height distribution of a specimen obtained in the form of a parabola based on theoretical equation (38) are in good agreement with the measured values.

b)The yield value, τ_{yF}, found from slump flow using theoretical equation (41) is in agreement with the yield value, τ_{yD}, found from the sphere drag test with an accuracy which is high enough for practical use.

This work clarifies the rheological significance of slump flow, and it is apparent that the yield value can be readily obtained from the slump flow.

(3) Future Problem

Theoretical equations (38) and (41) were derived from an equation that expresses the flow behavior of Bingham plastics, and the applicability of these theoretical equations to mortar which does not contain coarse aggregate was demonstrated. Although it might be assumed that concrete containing coarse aggregate can also be treated with these theoretical equations over the range in which its flow behavior matches that of Bingham plastics, the authors aim to carry out a verification of this as a future task.

The authors are also planning a study of the evaluation of plastic viscosity from the spreading rate of concrete in the slump flow test with the aid of the Equation (32), which was derived in the present study and expresses the flow behavior of concrete.

Acknowledgment

The authors would like to thank Prof. Shinobu Kakuta of Akashi Technical College for his helpful advice on the method of measurement of the rehological coefficients using a sphere viscometer.

References

1) Ozawa, K., Maekawa, K., and Okamura, H. : Development of the High Performance Concrete, *Proc. of JCI*, Vol.11, No.1, pp.699-704, 1989
2) Tattersall, G.H., and Banfill, P.F.G. : The Rheology of Fresh Concrete, *Pitman Advanced Publishing Program*, 1983
3) Kishitani, K., and Oka, S. : Rheological Measurement of Fresh Cement Paste and Mortar, *Transactions of AIJ*, No.305, pp.1-7, 1981.7
4) Murata, J., and Shimoyama, Y. : Deformation of Fresh Concrete under Static Load, *CAJ Proc. of Cement & Concrete*, No.30, pp.270-273, 1976
5) Mizuguchi, H. : Fundamental Study on Fluidity of Fresh Concrete, *Kyoto University*, 1984.2
6) Mori, H., and Tanigawa, Y. : Simulation of Flow Behavior of Fresh Concrete by Visco-plastic Element Analysis, *Transactions of AIJ*, No.374, pp.1-9, 1987.4
7) Kokado, T., and Hosoda, T. : Method of Evaluating Yield Value of Fresh Concrete with a Slump Flow Test, *Proc. of the 50th Annual Conference of JSCE*, Vol.V, pp.1002-1003, 1995.9
8) Fujiwara, H., Shimoyama, Y., and Endo, H. : Study on Evaluating Rheological Properties of Self-placing Concrete Mortar, *Proc. of the 49th Annual Conference of JSCE*, Vol.V, pp.306-307, 1994.9

9) Wylie, C.R. : Advanced Engineering Mathematics, *McGraw-Hill, Inc.*, pp.273*n*, 1962.5
10) JSCE : Guidelines for Measuring Properties of Fresh Concrete, *Proc. of the Symposium on Properties of Fresh Concrete and their Application in Concreting Practice*, pp.190-192, 1986.3
11) Yoshino, K. : Study on Evaluating Workability of High Flow Concrete, Nagoya University, pp.32-37, 1994
12) Kokado, T., and Miyake, M. : A Field Test on Deformable Concrete with Ground Granulated Blast-Furnace Slag, *Proc. of JCI*, Vol.13, No.1, pp.875-880, 1991
13) Kokado, T. : Materials for High-flow Concrete, *Concrete Journal*, Vol.32, No.7, pp.60-63, 1994.7
14) Ansley, R.W., and Smith, T.N. : Motion of Spherical Particles in a Bingham Plastic, *AIChE Journal*, Vol.13, No.6, pp.1193-1196, 1967.11